*33rd EPS Conference on Plasma Phys. Rome, 19 - 23 June 2006 ECA Vol.**30I**, P-1.012 (2006)*

Fast Electron Transport Measurements on the Vulcan PW Laser Facility

P.A.Norreys[1),2)], K.L.Lancaster[1)], J. S. Green[2)], C.D. Gregory[3)], K.U. Akli[4),5)], D.S. Hey[4),5)], J.R.Davies[6)], F.N. Beg[7)], S. Chen[7)], D. Clark[8)], R. Heathcote[1)], R. R. Freeman[8)], H. Habara[9)], K. Highbarger[8)], M. H. Key[5)], R. Kodama[9),10)], K. Krushelnick[2)], H.Nakamura[10)], M. Nakatsutsumi[9)], N. Patel[4)], F. Perez[4)], P.Simpson[11)], R. Stephens[12)], C. Stoeckl[13)], M. Storm[13)], M. Tampo[10)], W. Theobald[13)], R. Weber, M. S. Wei[7)], L. Van Woerkom[8)], N. Woolsey[3)], M.Zepf[11)]

1. CCLRC Rutherford Appleton Laboratory, Chilton, Didcot, Oxfordshire OX11 0QX, UK
2. Blackett Laboratory, Imperial College London, Prince Consort Road, London SW7 2BZ, UK
3. Department of Physics, University of York, York, Heslington, York YO10 5DD, UK
4. Department of Applied Sciences, UC Davis, 1 Shields Avenue, Davis, CA 95616-8254, USA
5. Lawrence Livermore National Laboratory, P.O. Box 808, Livermore, CA 94550, USA
6. GoLP/Centro de Fisica dos Plasmas, Instituto Superior Técnico, 1049-001 Lisbon, Portugal
7.Department of Mechanical and Aerospace Engineering, UC San Diego, 9500 Gilman Drive #0411, La Jolla, CA 92093-0411, USA
8. Department of Physics, Ohio State University, Columbus, Ohio, OH 43210-1117, USA
9. Graduate School of Engineering, Osaka University, Suita, 565-0871 Osaka, Japan
10. Institute of Laser Engineering, Osaka University, Suita, 565-0871 Osaka, Japan
11. Departments of Pure and Applied Physics, Queens University, Belfast BT7 1NN, UK
12. General Atomics, P.O. Box 86508, San Diego, CA 92186-5608, USA
13. Laboratory of Laser Energetics, University of Rochester, 250 East River Road, Rochester, NY 14623, USA

Significant progress has recently been made in understanding fast electron energy transport in solid density plasmas using the Vulcan 100 TW and PW facilities that have provided 0.5 ps – 1 ps laser pulses on target in the intensity regime 10^{19} Wcm^{-2} – 5×10^{20} Wcm^{-2}. We describe the different diagnostics employed and demonstrate that qualitative agreement has been found between the data from these experiments with analytic theory (the Davies' rigid beam model) and hybrid code modeling.

The essential ingredients of the rigid beam model are Ohm's law $E = \eta j_t$ that relates the electric field E to the current density j_t of the target, the target resistivity given by $\eta = \eta_0 (T/T_0)^{\alpha}$, where T is the temperature of the target, the subscript *0* indicates initial values and α is a constant, and Ohmic heating given by $\partial T/\partial t = \eta j_t / C$, where C is the heat

capacity. With the assumption of approximate (or quasi) current neutrality $j + j_t \approx 0$, Faraday's law provides the growth of the magnetic field

$$\frac{\partial \underline{B}}{\partial t} = \nabla \times \eta \underline{j} = \eta \nabla \times \underline{j} + \nabla \eta \times \underline{j} \qquad (1)$$

The first term on the right hand side of this equation generates a magnetic field that acts to push the electrons towards regions of high current density (providing a focusing or pinching effect) whereas the second term acts to push electrons towards regions of higher resistivity (providing a beam hollowing effect). Davies [1] solved this problem for a blunt cylindrical beam with a fixed current density moving at constant velocity that varies only with radius. He showed that, as the temperature rises, the magnetic field decreases and eventually changes sign, and hollows the beam rather than focus it.

We have recently reported new and significant observations of plasma formation on the back of thick plastic targets in multi-TW laser-plasma interactions where this effect is confirmed [2]. The experiments were performed with a series of higher laser powers than those used in the experiments that originally demonstrated magnetic focusing [3]. The results showed that, as the laser power increased, the jet from the back of the target became broader and was eventually replaced by a ring of plasma, in line with the predictions of this model.

To follow up these observations, we performed experiments to measure the beam divergence using the Vulcan PW laser facility. This laser delivers up to 300 J in pulse duration of 0.5 ps. Typically 40 % of the laser energy is contained within a 7 μm diameter focal spot, giving a focused intensity up to 5×10^{20} Wcm^{-2}. The p-polarized laser has a wavelength of 1054 nm and irradiated targets at 28° and 40° angle of incidence from the target normal. Copper targets of dimensions 4 mm × 2 mm ranging in thickness of 5 μm – 75 μm were irradiated. Up to 16 different diagnostics were employed on the experiments to measure the transport pattern . These included shadowgraphy and interferometry (using a 0.5 ps transverse probe beam), time resolved imaging of the thermal radiation in the optical region, 68 eV and 256 eV X-UV imaging using multi-layer mirrors with CCD detectors, Cu K_α X-ray imaging using spherically curved Quartz 211 crystals, X-ray pinhole cameras, single hit CCD spectrometers, conically curved CsAP spectrometers to measure the Al resonance line

emission spectra, and HOPG spectrometers. A schematic of the arrangement of some of these detectors is shown in Figure 1, along with typical images of the XUV and K_α signals that were recorded during the experiments [4].

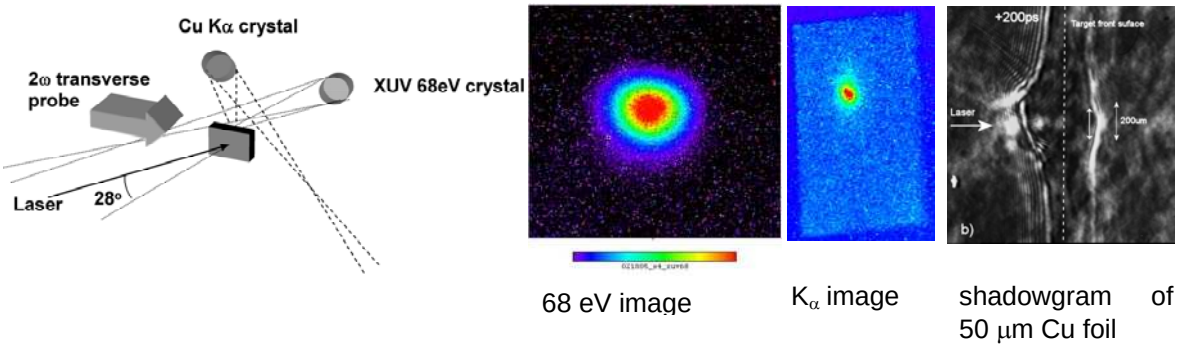

Figure 1. Schematic arrangement of the diagnostics and typical images obtained.

The diagnostics indicate a divergent energy flow pattern. The K_α imaging has a 54° angle compared with 78° for the shadowgrams. The shadowgrams are dependent on the expansion velocity of the plasma that, in turn, depends on a combination of energy density and mean kinetic energy of the fast electrons. The K_α imaging is dependent mainly upon the energy density of the fast electrons (and this explains the differences in the divergence angle derived from measurements using these diagnostic methods). The divergence angle is larger than the 40° reported by Stephens *et al.*, for lower intensities on target (that were up to 5×10^{19} Wcm^{-2}) [5]. The increased beam divergence with intensity on target is consistent with predictions of reduced magnetic focusing in the rigid beam model [6]. 5 μm Cu-foil targets show a "triple-humped" structure, but these are not due to beam hollowing. Instead, they are due to collisional filtering of lower energy electrons in the foil, resulting in a higher mean energy of the electrons emitted at large radii, which still had a sufficient energy density to form a plasma on the rear surface as a result of the high intensity and low target thickness. Most features of the experiment are qualitatively reproduced using the Davies' hybrid code, albeit with an upper and lower bound to the K_α divergence (which were limited by the particle boundary conditions in the code). These results have been submitted for publication [4].

Other targets were irradiated to investigate the effects of cone-guiding. Gold cones (40° opening angle, 30 μm inner end-wall diameter, 5 μm end-wall thickness) were attached to Al / Cu / Al slabs to diagnose energy transport through the package. Shadowgrams show large lateral expansion of the end of the cone, but no expansion on the rear surface of the diagnostic package. Thermal radiation from rear surface of the target shows little enhancement of the heating due to E-field and B-field guiding – the cone acts simply as additional material ρR. This may be due a number of factors – the cone angle, the end wall diameter being much larger than the focal spot (30 μm compared with 7 μm), the pedestal level etc. More experiments are needed before definite conclusions can be drawn.

Shadowgrams of cone-wire targets also show a large lateral plasma expansion around the tip of the cone. Hydrodynamic modelling of density profiles taken along different sections of the wire (derived from interferometry) indicates surface heating of the wires. See the paper by J.Green *et al.* in this conference proceedings.

Plastic cones (40° opening angle, 30 μm inner end-wall diameter, no end wall) were attached to 4 μm CH / 0.2 μm Al/ 4 μm CH slabs. The cone reduced the size of the heated region, although similar temperatures were derived from spectral line-shape fitting the Al He_α and Ly_α emission lines. It is interesting to note that the transport patterns changed from annular when plane plastic sandwich slab were irradiated to circular when cone-attached targets were irradiated. The 256 eV photon pattern is smaller in area with cone guide and close to the opening entrance hole diameter of the guide cone. The data is under analysis to model the interaction physics.

[1] J.R.Davies, Phys. Rev. E 68 056404 (2003)
[2] P.A.Norreys *et al.*, Plasma Phys. Controlled Fusion 48, L11 (2006)
[2] M.Tatarakis *et al.,* Phys. Rev. Lett. 81, 999 (1998)
[4] K.L.Lancaster *et al.,* Phys. Rev. Lett. (submitted for publication March 2006)
[5] R. B.Stephens *et al.*, Phys Rev E 69, 066414 (2004)
[6] J.R.Davies *et al.*, Plasma Phys. Controlled Fusion (submitted for publication April 2006)